Cell Reports, Volume *42*

Supplemental information

Neurons require glucose uptake and glycolysis *in vivo*

Huihui Li, Caroline Guglielmetti, Yoshitaka J. Sei, Misha Zilberter, Lydia M. Le Page, Lauren Shields, Joyce Yang, Kevin Nguyen, Brice Tiret, Xiao Gao, Neal Bennett, Iris Lo, Talya L. Dayton, Martin Kampmann, Yadong Huang, Jeffrey C. Rathmell, Matthew Vander Heiden, Myriam M. Chaumeil, and Ken Nakamura

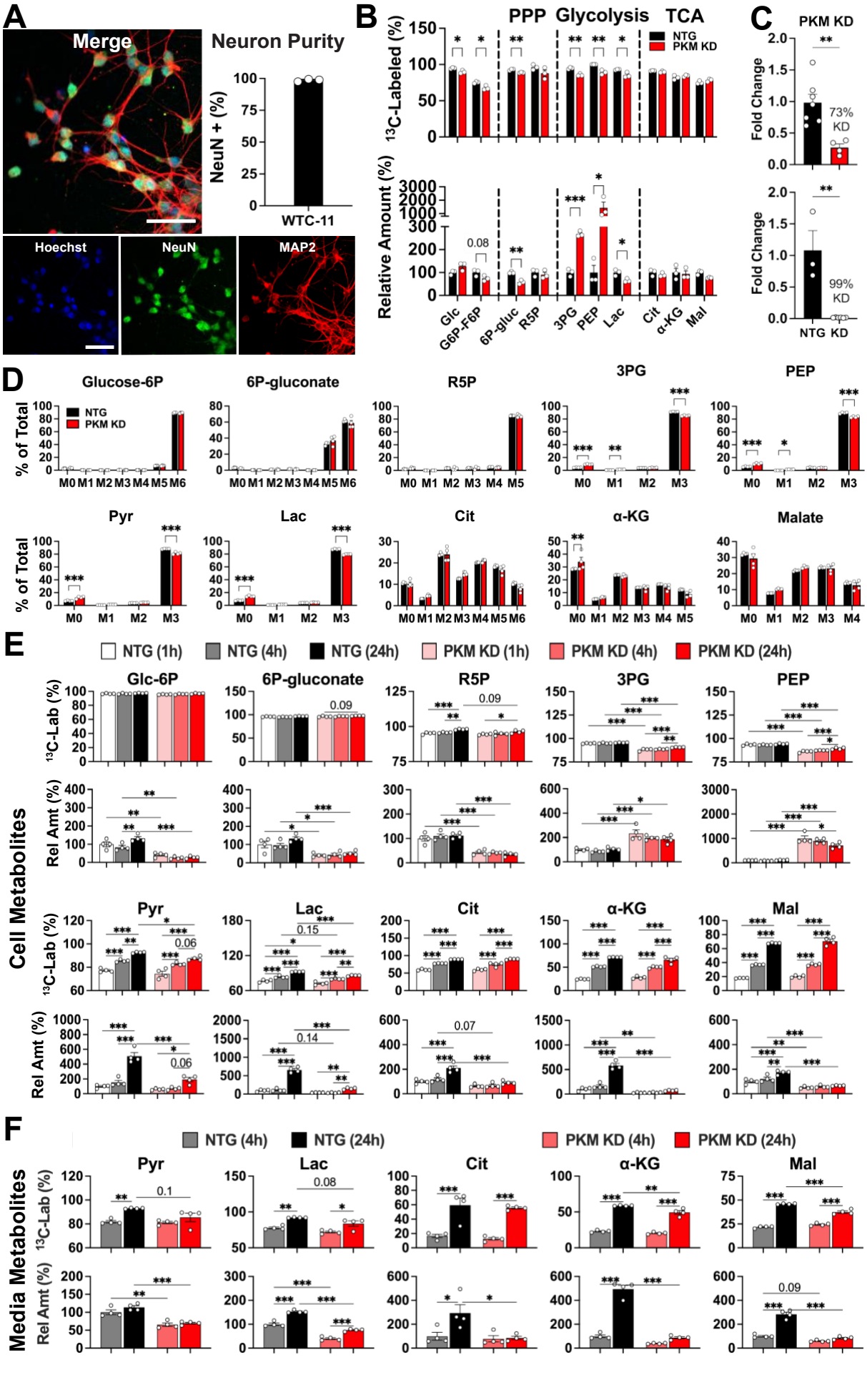
A
Merge
Neuron Purity
NeuN + (%)
WTC-11
Hoechst
NeuN
MAP2
B
PPP Glycolysis TCA
NTG
PKM KD
13C-Labeled (%)
Relative Amount (%)
Glc
G6P-F6P
6P-gluc
R5P
3PG
PEP
Lac
Cit
α-KG
Mal
0.08
C
PKM KD
Fold Change
73% KD
99% KD
NTG KD
D
Glucose-6P
6P-gluconate
R5P
3PG
PEP
Pyr
Lac
Cit
α-KG
Malate
% of Total
E
NTG (1h)
NTG (4h)
NTG (24h)
PKM KD (1h)
PKM KD (4h)
PKM KD (24h)
Glc-6P
6P-gluconate
R5P
3PG
PEP
Cell Metabolites
13C-Lab (%)
Rel Amt (%)
Pyr
Lac
Cit
α-KG
Mal
F
Media Metabolites

Figure S1. iPSC neurons depend on glycolysis to metabolize glucose. Related to Figure 1.
(A) iPSCs differentiated into neurons for 12 days stained for MAP2 (red), NeuN (green) and Hoechst (blue). Scale bar is 50 μm. Purity of neuronal culture measured by % overlap of NeuN on DAPI derived from n = 3 coverslips each compiled from 3 fields with 90-300 cells/field.
(B) Cellular metabolites showing fractional abundance of ^{13}C (top) and total relative metabolite levels (bottom) between PKM KD (99% KD efficiency) and NTG iPSC-derived neurons. Identical NTG controls (20.5 mM [U-^{13}C]glucose) are shown in Figure S7B. n = 3 samples/group.
(C) Knockdown of PKM expression in PKM KD versus NTG neurons used in experiment 1 (Figures 1A, 1B, and S1D-F, top) and experiment 2 (Figure S1B, bottom). Experiment 1 used PKM KD cells from 3 later passages than what was used in experiment 2, and had somewhat reduced knockdown. n = 3-7 samples/group.
(D) Isotopologue fractions for cellular PPP, glycolytic, and TCA cycle metabolites derived from [U-^{13}C]glucose incubated with NTG and PKM KD neurons with 73% KD efficiency for 24 hours. n = 4 samples/group.
(E, F) Metabolite amounts and [U-^{13}C]glucose fractional labeling derived from (E) cells at 1 hour, 4 hours, and 24 hours and from (F) media at 4 hours and 24 hours using PKM KD neurons with 73% KD efficiency. n = 4 samples/group.
*****p<0.05, **p<0.01, ***p<0.001 by unpaired t-tests (B, C) and *p<0.05, **p<0.01, ***p<0.001 by two-way ANOVA with Sidak's multiple comparison test (D-G).

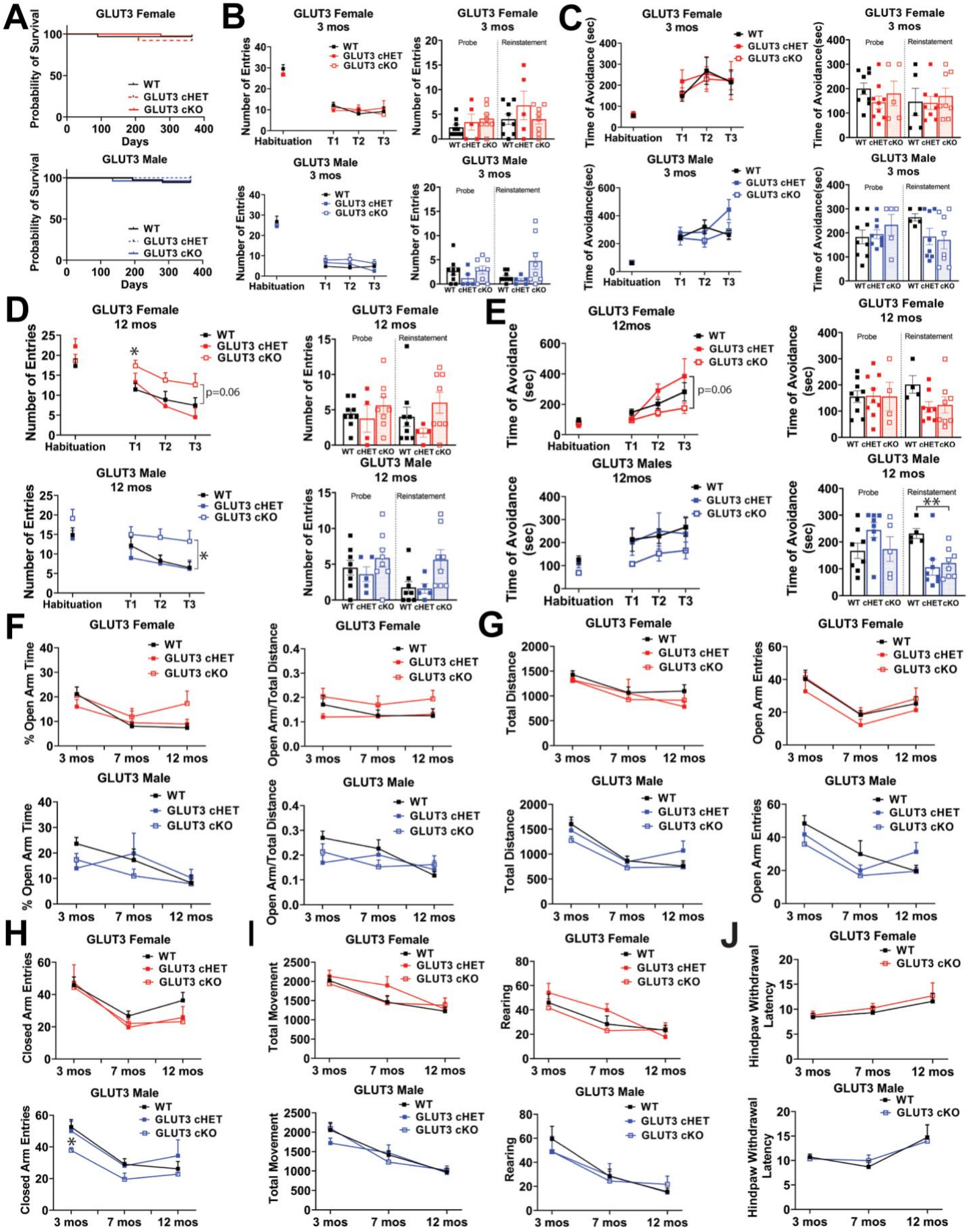

Figure S2. GLUT3 cKO mice have impaired spatial learning and memory. Related to Figure 2.

(A) Kaplan–Meier survival curve of GLUT3cKO, GLUT3 HET and wild-type mice, separated by sex. GLUT3 cKO mice had normal survival compared to controls through 12 months of age.
GLUT3cKO (n = 42 female, 27 male), GLUT3 Het (n = 13 female, 15 male) and control (n = 33 female, 37 male), no significant changes in GLUT3cKO versus control mice by log-rank (Mantel-Cox) test.
(B-E) Mice were assessed for spatial learning and memory with the active place avoidance test, separated by sex. Habituation to the apparatus was performed ahead of training trials 1–3 (T), followed by a probe trial, and a reinstatement trial. Number of entrances into the aversive zone and maximal time of avoidance of this zone were used as the main outcome parameters. GLUT3cKO, GLUT3 HET and wild-type mice performed similarly at 3 months-of-age (B,C). However, at 7 months (Figure 2) and 12 months (D,E) both sexes of GLUT3cKO mice showed elevated numbers of entries into the aversive zone and decreased maximal avoidance time versus controls. Data are means ± SEM; n = 5-9 mice/group complied from three cohorts.
(F- H) Elevated Plus Maze Testing of GLUT3cKO, GLUT3 HET and wild-type mice at 3, 7 and 12 months of age. There were no significant differences in %open arm time and open arm/total distance (F), total distance and open arm entries (G), or closed arm entries (H).
(I) No differences in total movement or rearing were detected in open field test.
(**J**) Hot plate test. No differences in hindpaw withdrawal were detected.
*p<0.05, **p<0.01 by Welch ANOVA with Dunnett's T3 multiple comparisons test. Brackets in graphs show significance of linear mixed modeling for genotype (D,E).

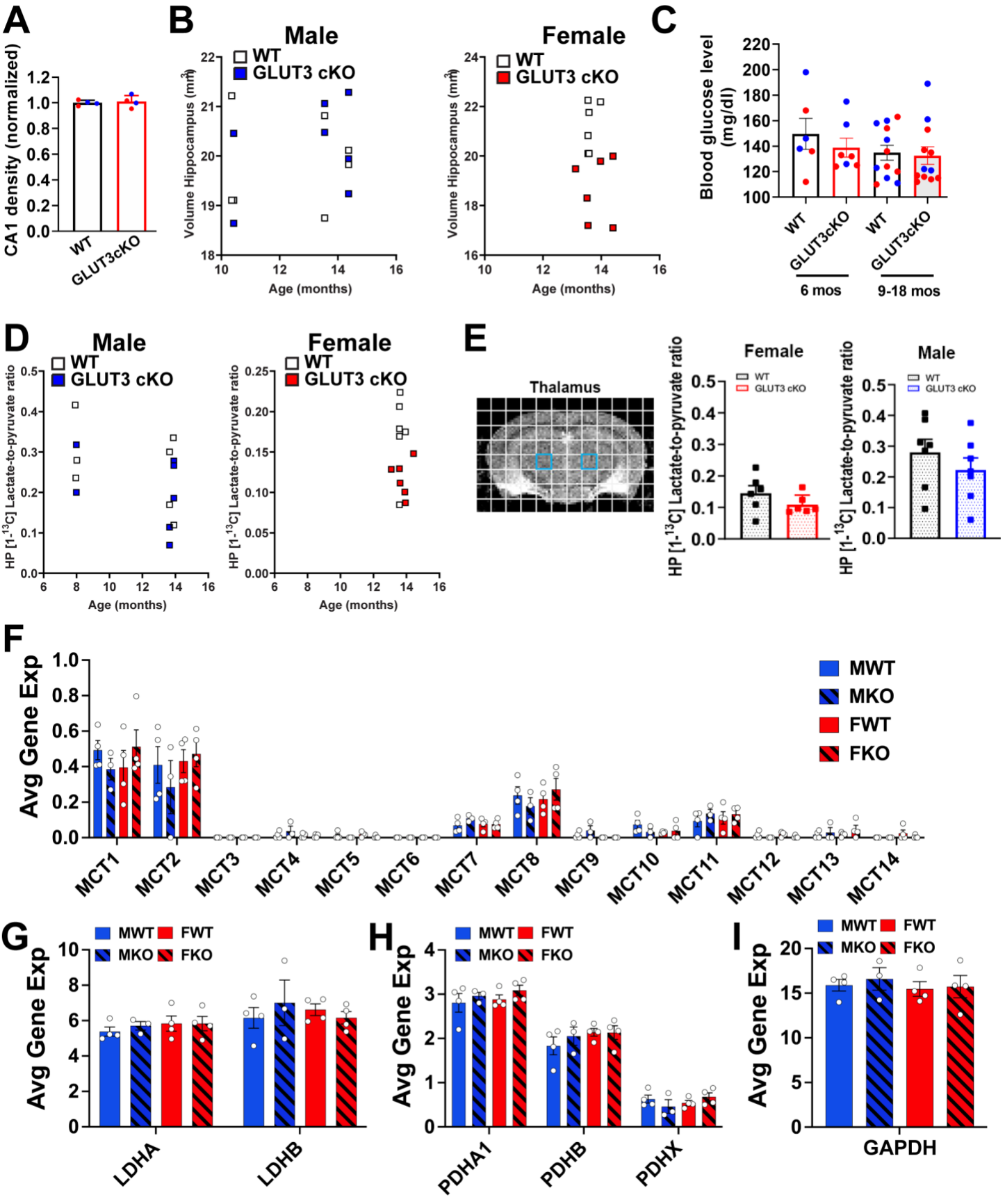

Figure S3. Pyruvate metabolism is unaffected in GLUT3cKO mice. Related to Figure 3.
(A) GLUT3cKO had no effect on the density of CA1 neurons in 15 month-old-mice. Data are means ± SEM. n = 4 mice/group, from 2 slices/mouse, 4-8 images/slice.
(B) T_2 weighted image estimates for hippocampal volume versus age. n=6-7 mice/group/sex.

(C) GLUT3cKO had no effect on blood glucose levels. n = 3-4 mice/group/sex at 6 months-of-age; n = 4-8 mice/group/sex at 12-18 months-of-age for males (blue dots) and females (red dots).
(D) Hippocampal HP [1-^{13}C] Lactate-to-pyruvate ratio versus age. n=6-7 mice/group per sex.
(E) *In vivo* metabolic MRI from thalamus of 8 to 14-month-old mice. GLUT3cKO had no effect on HP [1-^{13}C] lactate-to-pyruvate ratios in the thalamus (blue squares) in either male or female mice. Dots represents value obtained for each individual. n=6-7 mice/group per sex.
(F-I) GLUT3cKO does not impact expression of (F) MCT, (G) LDH or (H) PDH. (I) GAPDH in CA1 neurons. n = 3-4 mice/group compiled from 20-36 (CA1) capture areas/region.
Not significant by unpaired t-tests (A, C, E), multiple linear regression analysis (B, D), two-way ANOVA with Sidak's multiple comparisons test (F-H), one-way ANOVA with Sidak's multiple comparisons test (I).

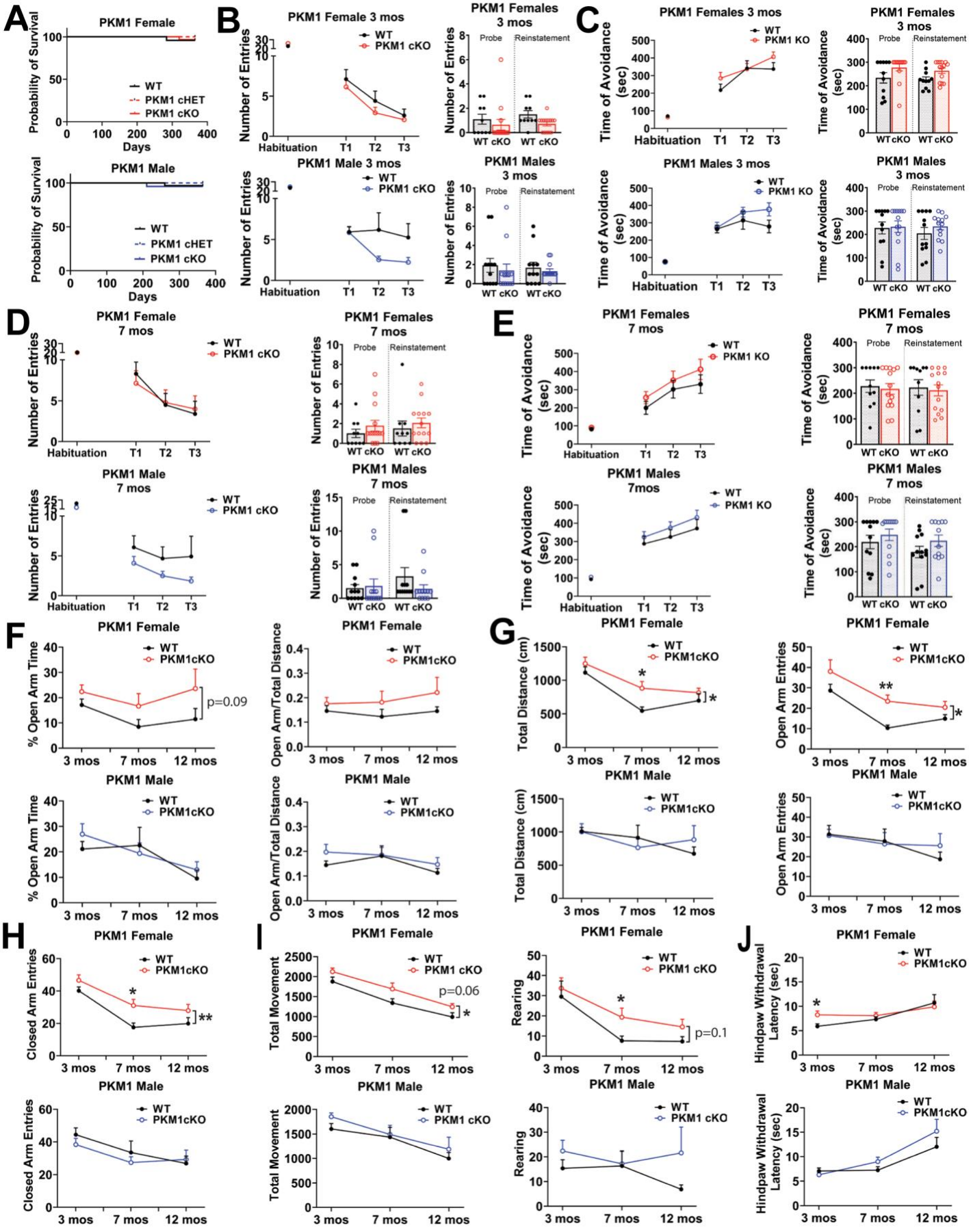
A
PKM1 Female
Probability of Survival
Days
WT
PKM1 cHET
PKM1 cKO
PKM1 Male
B
PKM1 Female 3 mos
Number of Entries
Habituation
T1
T2
T3
PKM1 Females 3 mos
Probe
Reinstatement
WT cKO
PKM1 Male 3 mos
PKM1 Males 3 mos
C
PKM1 Females 3 mos
Time of Avoidance (sec)
PKM1 KO
PKM1 Males 3 mos
D
PKM1 Female 7 mos
PKM1 Male 7 mos
PKM1 Females 7 mos
PKM1 Males 7 mos
E
PKM1 Females 7 mos
PKM1 Males 7mos
F
PKM1 Female
% Open Arm Time
PKM1cKO
3 mos
7 mos
12 mos
p=0.09
PKM1 Male
Open Arm/Total Distance
G
Total Distance (cm)
Open Arm Entries
H
Closed Arm Entries
I
Total Movement
Rearing
p=0.06
p=0.1
J
Hindpaw Withdrawal Latency (sec)

Figure S4. Female PKM1cKO mice develop hyperactivity prior to spatial learning and memory deficits. Related to Figure 4.

(A) Kaplan–Meier survival curve of PKM1 cKO and wild-type mice, separated by sex. PKM1 cKO mice had normal survival compared to controls through 12 months of age. PKM1cKO (n = 30 female, 25 male), PKM1 Het (n = 14 female, 16 male) and PKM1 (n = 24 female, 32 male), not significant by log-rank (Mantel-Cox) test.

(B-E) Mice were assessed for spatial learning and memory with the active place avoidance test, separated by sex. Habituation to the apparatus was performed ahead of training trials 1–3 (T), followed by a probe trial, and a reinstatement trial. Number of entrances into the aversive zone and maximal time of avoidance of this zone were used as the main outcome parameters. PKM1 cKO and wild-type mice performed similarly at 3 and 7 months-of-age.

(F-H) Behavioral responses of PKM1 cKO, and wild-type mice in elevated plus Maze testing at 3, 7 and 12 months of age. PKM1cKO female mice had increased open arm entries, increased total distance (G), and increased closed arm entries (H), as well a trend for increased open arm time (F). PKM1cKO male mice don't show significant differences.

(I) PKM1cKO female mice have exhibit increased total movement and rearing in open field test, whereas no change were observed in PKM1cKO male mice.

(**J**) Hot plate test. No differences in hindpaw withdrawal were detected.

*p<0.05 **p<0.01 by Welch's t-test (G,H,I,J). Brackets in graphs show significance of linear mixed modeling for genotype (F,G,H,I).

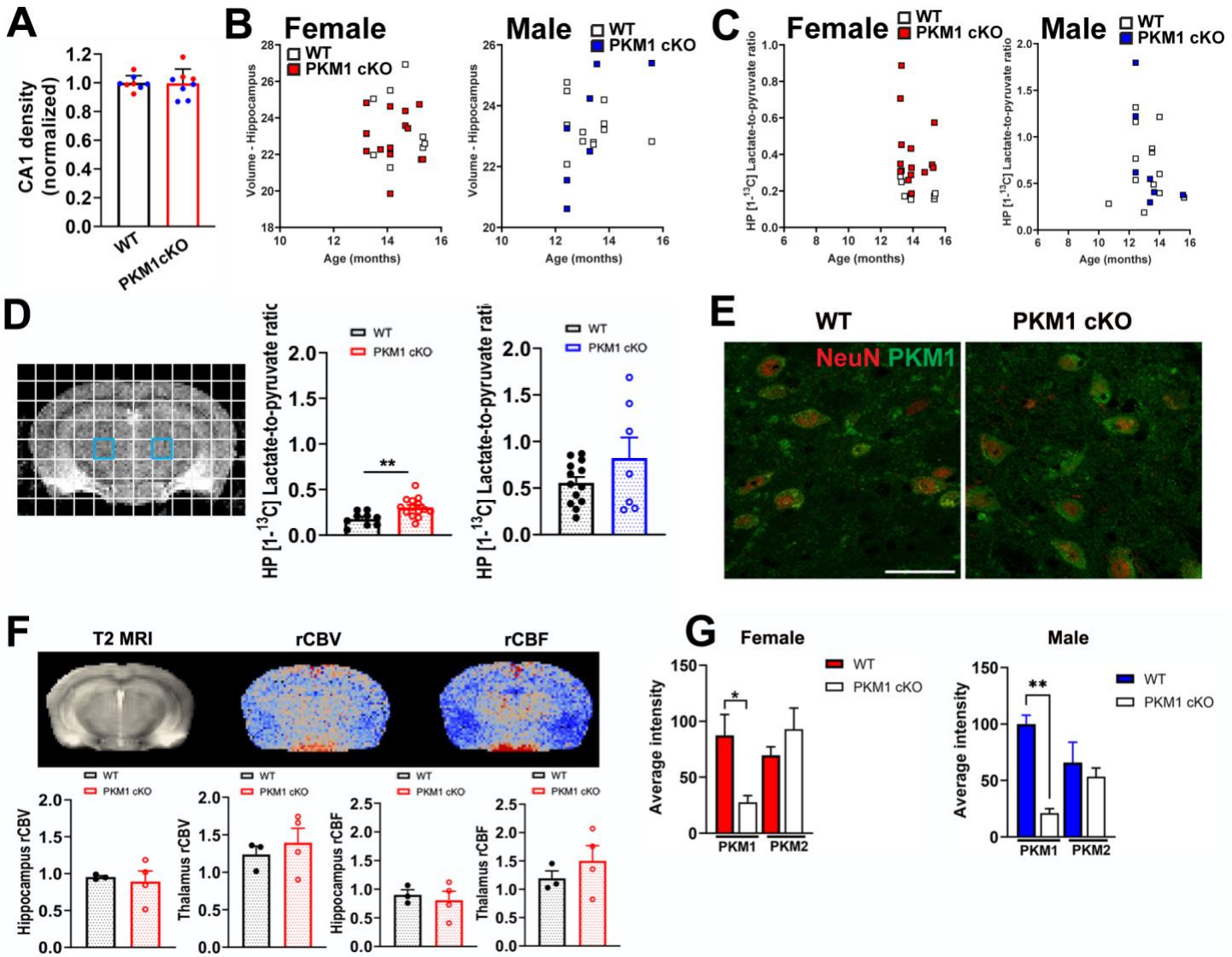

Figure S5. PKM1cKO mice have altered pyruvate to lactate conversion in areas lacking PKM1 deletion, despite normal neuronal density, cerebral perfusion and PKM2 levels. Related to Figure 5.

(A) PKM1cKO had no effect on the density of CA1 neurons in 14 month-old-mice. Data are means ± SEM, n = 7-8 mice/group, from 2 slices/mouse, 4-8 images/slice. The blue dots represent males and the red dots represent females.

(B) Volume of the hippocampus estimated from *in vivo* T_2 weighted images versus age for PKM1WT and PKM1cKO mice, n=9 female PKM1WT, 14 female PKM1cKO, 7 male PKM1WT, 13 male PKM1cKO.

(C) Hippocampal HP [1-^{13}C] Lactate-to-pyruvate ratio versus age for PKM1WT and PKM1cKO mice. n = 9 female PKM1WT, 14 female PKM1cKO, 7 male PKM1WT, 13 male PKM1cKO.

(D) *In vivo* metabolic MRI from thalamus of 11 to 15-month-old mice. PKM1cKO increased HP [1-^{13}C] lactate-to-pyruvate ratios in the thalamus (blue squares) in female mice, while no significant effect was detected in males. N = 9 female PKM1WT, N = 14 female PKM1cKO, N = 7 male PKM1WT, N = 13 male PKM1cKO.

(E) Representative images from thalamus of 12-month-old PKM1 cKO and PKM1 WT mice, shows immunofluorescence for NeuN (red) and PKM1 (green). The scale bar is 40 □m.

(F) Dynamic susceptibility contrast imaging of 16 to 17-month-old mice. Representative T_2 weighted MR image and relative cerebral blood volume (rCBV) and cerebral blood flow (rCBF) maps. There were no significant difference in either rCBV or rCBF between female PKM1WT and PKM1cKO mice in the hippocampus or thalamus. Data are shown as mean±S.E.M. N = 3 female PKM1WT, N = 4 female PKM1cKO.

(G) Hippocampal slices from 12-14 months old PKM1cKO and control mice were stained against PKM1 and PKM2. PKM1 staining is markedly decreased in CA1 neurons in PKM1KO male and female, while PKM2 levels not changed. n = 2 female PKM1WT, 2 female PKM1cKO, 2 male PKM1 WT and 2 male PKM1cKO. 2-4 slices/mouse, 4-8 cells/slice from 3 independent experiments.

ns = Not significant, *p<0.05 , **p<0.01 by unpaired t-test (A, D, F), multiple linear regression analysis (B, C), and one- way ANOVA with Sidak's multiple comparisons test (G).

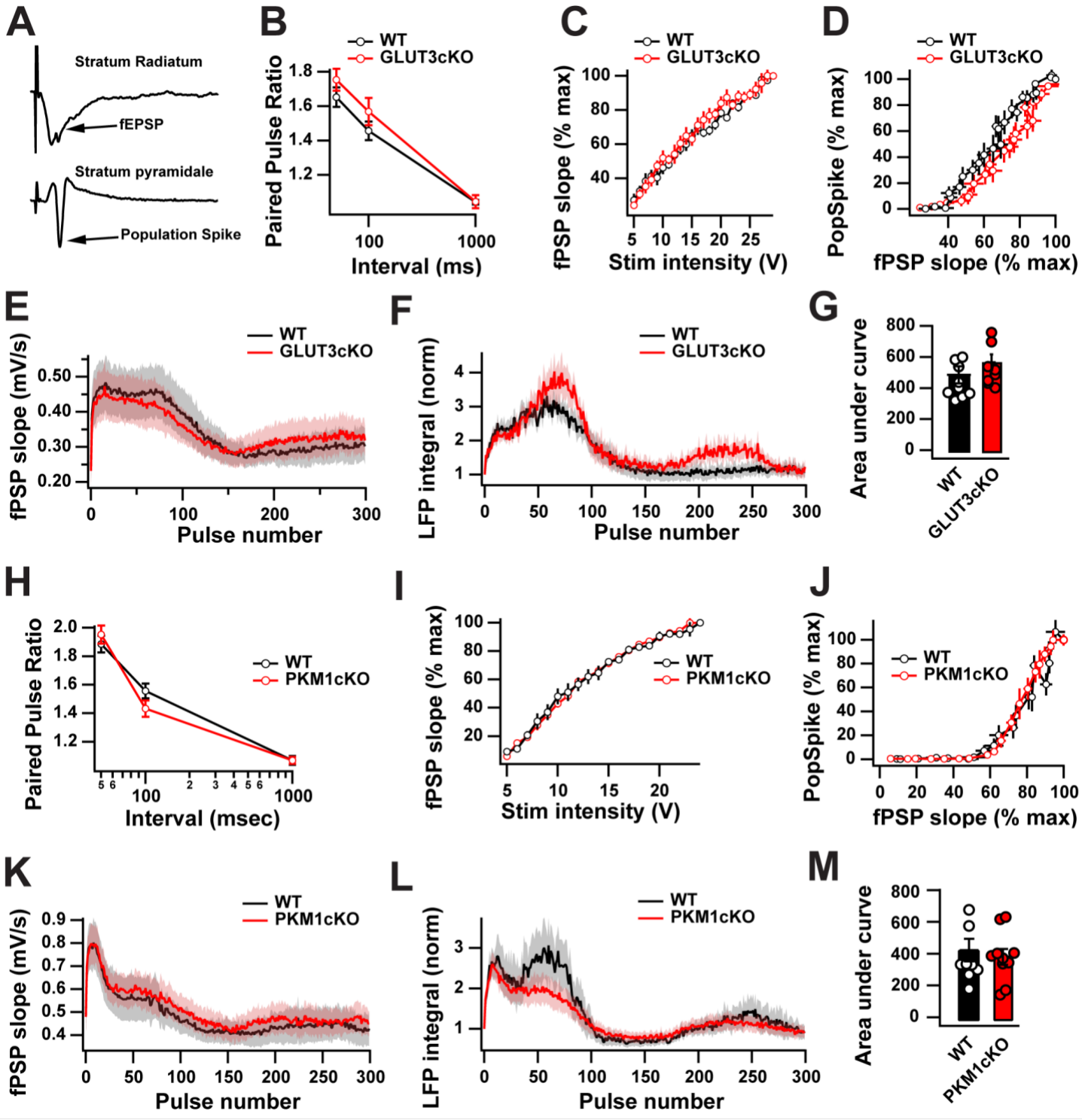

Figure S6. GLUT3cKO and PKM1cKO do not impact the post-synaptic function of CA1 neurons in acute hippocampal slices. Related to STAR Methods.

(A) Sample local field potential (LFP) response to a single Schaffer collateral stimulation recorded simultaneously from stratum Radiatum (top) and stratum Pyramidale (bottom) of CA1 region in acute hippocampal slices.

(B,H) Mean paired-pulse ratio values for three interpulse intervals for WT (black) and KO (red).

(C,I) Normalized fPSP slope values under increasing synaptic stimulation intensity.

(D,J) CA1 excitability represented as population spike (PopSpike) integral in response to increasing synaptic stimulation (fPSP slope).

(E-G) Unchanged network function during repetitive synaptic stimulation. Network activity was induced by 10Hz, 30-sec (300 pulse) Schaffer collateral stimulation and recorded both as fPSPs (stratum radiatum) and population activity (stratum pyramidale).
(E,K) Individual fPSP slope values for each stimulation pulse in the train both for WT (black) and KO (red) slices.
(F,L) LFP integrals in stratum pyramidale, normalized to 1st pulse LFP integral.
(G,M) Area under curve (AUC) values for train LFP integrals in (F,L) for all experiments.
Data are means ± SEM. (B-G), n = 10 slices PKM1cKO, 9 slices PKM1wt, both compiled from two mice per group. (H-M), n = 10 slices for both GLUT3cKO and WT, from two mice per group. No significant differences by Mann-Whitney U test.

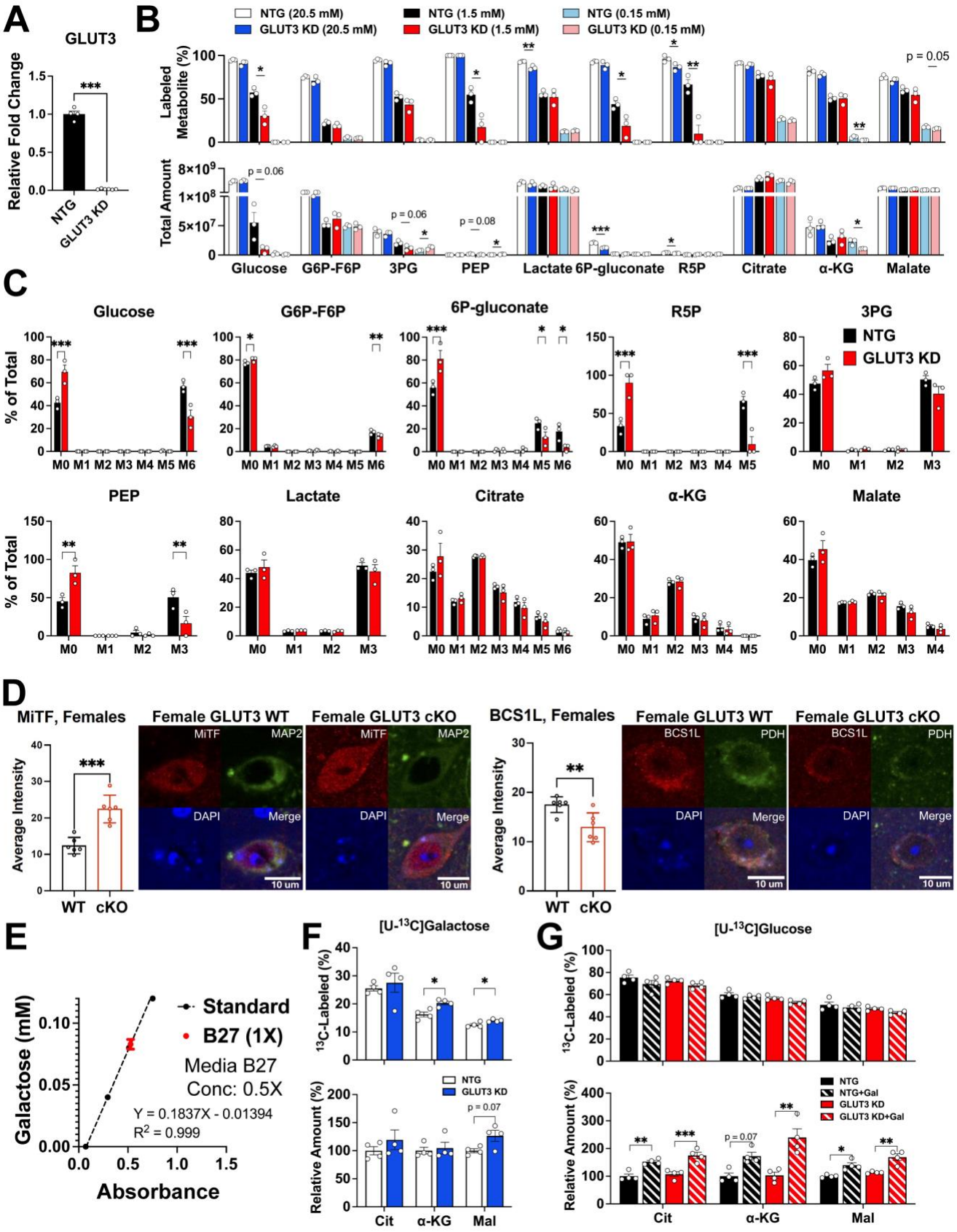

Figure S7. Impact of GLUT3 loss on glucose metabolism and mitochondrial gene expression. Related to Figures 6 and 7.

(A) Fold change and knockdown of GLUT3 expression for non-target and GLUT3 KD iPSC neurons differentiated for 12 days. Data shows mean ± SEM. n = 3 samples/group.

(B) Metabolomics of non-target and GLUT3 KD neurons incubated with 0.15 mM, 1.5 mM, and 20.5 mM of [U-^{13}C]glucose for 24 hours. Identical NTG controls (1.5 mM [U-^{13}C]glucose) are shown in Figures 6B and S7C. Identical NTG controls (20.5 mM [U-^{13}C]glucose) are shown in Figure S1B. n = 3 samples/group.
(C) Isotopologue fractions for select metabolites comparing NTG and GLUT3 KD iPSC neurons differentiated for 12 days. n = 3 samples/group. Identical NTG controls (1.5 mM [U-^{13}C]glucose) are shown in Figures 6B and S7B.
(D) Cytosolic immunofluorescence of Mitf and BCS1L in neurons from GLUT3 KO females. n = 6 sections across 3 mice/group. BCS1L (WT n = 78 total neurons; KO n = 73), Mitf (WT n = 81; KO n = 76). Scale bar is 10 μm.
(E) Colorimetric measurements of galactose levels in neuronal differentiation media containing B27 supplement. n = 3 samples/group.
(F) Relative total amounts and [U-^{13}C]galactose fractional labeling of TCA cycle metabolites in GLUT3 KD and NTG neurons after 24 hours of culture. n = 4 wells/group.
(G) Relative total amounts and [U-^{13}C]glucose fractional labeling of the TCA cycle metabolites in GLUT3 KD neurons relative to NTG neurons when treated with either 1.5 mM of [U-^{13}C]glucose or 1.5:1.5 mM [U-^{13}C]glucose:galactose for 24 hours. n = 4 samples/group.
Data are means ± SEM. *p<0.05, **p<0.01, and ***p<0.001 by unpaired t-tests (A), two-way ANOVA with Sidak's multiple comparisons test (B, C, G), and unpaired t-test (F).
See also Tables S5 and S7.

Number of Capture Areas	CA1	CA3	Dentate Gyrus (DG)	Thalamus (TH)
Mean	28.3	21.8	23.4	117.9
Standard Dev.	8.0	9.0	10.2	53.0

Table S1. Average number of RNA capture areas in Visium. Related to Figures 2, 7, and S3. Male WT (n = 4 mice), Male GLUT3 cKO (n = 3), Female WT (n = 4), Female GLUT3 cKO (n = 4). Anatomical regions include CA1, CA3, Dentate Gyrus (DG), and Thalamus (TH).

Gene Ontology Term	**P-value**
negative regulation of cellular respiration (GO:1901856)	0.003
non-canonical Wnt signaling pathway via MAPK cascade (GO:0038030)	0.003
positive regulation of mitochondrial depolarization (GO:0051901)	0.003
galactose catabolic process (GO:0019388)	0.004
sialylation (GO:0097503)	0.004
glycoside metabolic process (GO:0016137)	0.004
glycosyl compound catabolic process (GO:1901658)	0.004
glycosylceramide catabolic process (GO:0046477)	0.004
glycosylceramide metabolic process (GO:0006677)	0.004
regulation of macromolecule biosynthetic process (GO:0010556)	0.004

Table S2. Enrichment of Gene Ontology terms and their respective p-values from Enrichr. Related to Figure 7. The top 10 terms derived from the top 20% of differentially expressed genes in CA1 neurons between GLUT3cKO and WT mice from Visium are shown.

Table S3. Visium-derived gene expression values for the mouse transcriptome between GLUT3 cKO mice and WT mice for males and females in CA1. Related to Figures 2, 7, and S3. Male WT (n = 4), Male GLUT3 cKO (n = 3), Female WT (n = 4), Female GLUT3 cKO n = 4).

Table S4. Visium-derived gene expression values for the mouse transcriptome between GLUT3 cKO mice and WT mice for males and females in the thalamus. Related to Figures 2, 7, and S3. Male WT (n = 4), Male GLUT3 cKO (n = 3), Female WT (n = 4), Female GLUT3 cKO (n = 4).

Table S5. UPLC-MS derived mass spectra peak areas for metabolite isotopologues. Related to Figures 6, S1, and S7. Non-target (NTG) vs GLUT3 KD at 20.5 mM [U-^{13}C]glucose metabolite amounts were used for Figure S7. NTG vs PKM KD at 20.5 mM [U-^{13}C]glucose was used for Figure S1. The 20.5 mM [U-^{13}C]glucose condition was applied for 24 hours. GLUT3 KD neurons were also compared to NTG neurons with 1.5 mM and 0.15 mM glucose at 1 and 24 hours of incubation as plotted in Figures 6 and S7. n = 3 samples/group.

Table S6. IC-MS derived mass spectra peak areas for metabolite isotopologues for PKM KD, non-target (NTG) neurons, and their respective medias. Related to Figures 1 and S1. Neurons were given [U-^{13}C]glucose at 20.5 mM for 1, 4, and 24 hours. Media samples were collected at 4 and 24 hours. n = 4 samples/group.

Table S7. IC-MS derived mass spectra peak areas for metabolite isotopologues for GLUT3 KD and non-target (NTG) neurons in various glucose/galactose conditions. Related to Figures 7 and S7. Neurons were given media containing 1.5 mM of either [U-^{13}C]glucose, equimolar amounts of [U-^{13}C]glucose and galactose, or just [U-13C]galactose for 24 hours. n = 4 samples/group.